SCIENTIFIC REPORTS

OPEN

SUBJECT AREAS:
CONDENSED-MATTER PHYSICS
SOLID-STATE CHEMISTRY
STRUCTURE OF SOLIDS AND LIQUIDS
FERROELECTRICS AND MULTIFERROICS

Received
21 March 2013

Accepted
31 July 2013

Published
16 August 2013

Correspondence and requests for materials should be addressed to J.C. (junchen@ustb.edu.cn) or X.R.X. (xing@ustb.edu.cn)

Effectively control negative thermal expansion of single-phase ferroelectrics of $PbTiO_3$-$(Bi,La)FeO_3$ over a giant range

Jun Chen[1,2], Fangfang Wang[1], Qingzhen Huang[3], Lei Hu[1], Xiping Song[4], Jinxia Deng[1], Ranbo Yu[1] & Xianran Xing[1,2]

[1]Department of Physical Chemistry, University of Science and Technology Beijing, Beijing 100083, China, [2]State Key Laboratory for Advanced Metallurgy, University of Science and Technology Beijing, Beijing 100083, China, [3]NIST Center for Neutron Research, National Institute of Standards and Technology, Gaithersburg MD, 20899-6102, USA, [4]State Key Laboratory for Advanced Metals and Materials, University of Science and Technology Beijing, Beijing 100083, China.

Control of negative thermal expansion is a fundamentally interesting topic in the negative thermal expansion materials in order for the future applications. However, it is a challenge to control the negative thermal expansion in individual pure materials over a large scale. Here, we report an effective way to control the coefficient of thermal expansion from a giant negative to a near zero thermal expansion by means of adjusting the spontaneous volume ferroelectrostriction (SVFS) in the system of $PbTiO_3$-$(Bi,La)FeO_3$ ferroelectrics. The adjustable range of thermal expansion contains most negative thermal expansion materials. The abnormal property of negative or zero thermal expansion previously observed in ferroelectrics is well understood according to the present new concept of spontaneous volume ferroelectrostriction. The present studies could be useful to control of thermal expansion of ferroelectrics, and could be extended to multiferroic materials whose properties of both ferroelectricity and magnetism are coupled with thermal expansion.

The thermal expansion compatibility of different component is a one of key problems for modern devices, such as thin film, multilayer chip capacitors (MLCCs), solid oxide fuel cell (SOFC), thermoelectric materials, and high temperature piezoelectrics[1–4]. Thermal stress could give rise to material failure due to undesirable mismatch of coefficient of thermal expansion (CTE) of different components. The control of thermal expansion is an important topic for the material design. Negative thermal expansion (NTE) was recently found in some materials in the past two decades[5–11]. NTE materials have a promising potential application on tailoring CTE[7]. The overall thermal expansion can be tailored by either formation of composites or chemical modification of single-phase materials. For example, some composites were fabricated, such as ZrW_2O_8 with common materials[12,13]. The progress is, however, hampered mainly due to the poor thermal stability of ZrW_2O_8. It decomposes at a relatively low temperature (777°C)[7]. If the control of CTE could be achieved in single-phase materials, drawbacks in composites such as low binding capacity, thermal stress, or chemical reaction at interface, could be effectively overcame.

The control of NTE is an interesting topic for the studies on NTE especially of individual pure materials. Many kinds of chemical modifications have been carried out on various NTE materials. For example, ZrW_2O_8 based single-phase materials show little dependence of NTE on compositions and behave a very small varied range of CTE ($\alpha_V = -2.2 \sim -2.6 \times 10^{-5}{}^{\circ}C^{-1}$) by chemical modifications[14]. The control of NTE of ZrW_2O_8 is restricted by the fact of few suitable substitutions and low solubility limit. A single-phase ceramic material of $Al_{2x}(Hf,Mg)_{1-x}(WO_4)_3$ was found to have a bulk CTE range of $-0.23 \sim 0.45 \times 10^{-5}{}^{\circ}C^{-1}$, where a zero thermal expansion (ZTE) was also achieved[8]. Orthophosphate group of $NaZr_2(PO_4)_3$ (NZP) of fast ionic conductivity have been widely studied with various substitutions at different sites to exhibit a CTE range of $-0.17 \sim 0.19 \times 10^{-5}{}^{\circ}C^{-1}$[15]. The effect of cation size could play an important role in the thermal expansion property of NZP-based materials[16]. More recently, anti-perovskite Mn_3AN (A = Zn and Ga) nitrides were found to have a giant NTE which was suggested to correlate with the coupling between the Γ^{5g} antiferromagnetic spin configuration and lattice[17,18]. Many kinds of substitutions have been tried at three crystallographic sites in order for adjusting thermal expansion of Mn_3AN. ZTE could be established in, for example, nanocrystalline $Mn_3Cu_{0.5}Ge_{0.5}N$ below -55 °C[19], and $Mn_3(Ga_{0.5}Ge_{0.4}Mn_{0.1})(N_{1-x}C_x)$ in a temperature range of $-83 \sim 0$ °C[20]. The further studies on the complex interplay between magnetic exchange, cation radius, and lattice would allow more precisely control NTE

of Mn_3AN materials, especially for a wide temperature range. The challenge still remains for the control of single-phase NTE materials. Especially, the control of NTE over a large range would benefit the practical applications of NTE materials.

Among the family of NTE materials, there is one branch of ferroelectrics which behave a general phenomenon that unit cell volume contracts during ferroelectric-to-paraelectric phase transition, such as perovskites of $PbTiO_3$ (PT)[21–23], $BaTiO_3$[24], $BiFeO_3$[25], and (Bi,La)NiO_3[9], tungsten bronze $PbNb_2O_6$[26], and semiconductor GeTe[27]. It is important to note that all ferroelectrics except PT (RT $\sim$ 490°C)[23] exhibit NTE property within a narrow temperature range, e.g. 50°C for $BiFeO_3$[25]. Such large NTE temperature range of PT offers us an opportunity to control the NTE property. Our previous studies have revealed that the CTE can be adjusted by chemical substitutions for either Pb or Ti cations[21–23]. The temperature dependence of spontaneous polarization (P_S) and lattice dynamics have approved that the ferroelectric behaviour plays an important role in the NTE nature of PT-based materials[21,22]. For future application of the NTE PT-based materials, however, one of main problems still remains. That is how to easily control the NTE over a large scale. Here, we report an effective way to control the NTE of ferroelectrics over a giant scale through a simple method by adjusting the ratio of cations with different ferroelectric activity which is defined as the P_S displacement in the oxygen polyhedron[28,29]. The proposed system is the $0.5PbTiO_3$-$0.5(Bi_{1-x}La_x)FeO_3$ (abbreviated as the 0.5PT-0.5BL$_x$F, $0.0 \leq x \leq 0.2$) whose Bi and La have essentially the same cation radius (1.34 Å for Bi^{3+} and 1.36 Å for La^{3+}) however with much different ferroelectricity activity. Bi^{3+} has the strongest ferroelectric activity (0.8Å), while La^{3+} has the weakest one (0.05Å)[28,29]. The average bulk CTE can be controlled over a giant range from -7.0 to -0.71×10^{-5}°C^{-1}, which contains most known NTE materials. The detailed structure was investigated by both neutron powder diffraction based on Rietveld refinement and density function theory (DFT) calculation. A new concept of spontaneous volume ferroelectrostriction (SVFS) is proposed to elucidate the mechanism of NTE control in ferroelectrics.

Results

It is known that (1-x)$PbTiO_3$-$x$$BiFeO_3$ binary system can form a full range solid solution with a morphotropic phase boundary (MPB) around at $x = 0.65$, and exhibits unusual physical properties of much enhanced c/a, NTE, and Curie temperature (T_C)[23,30,31]. As the $x = 0.0$ for the 0.5PT-0.5BL$_x$F, the c/a is significantly enhanced to 1.14 when compared with PT (c/a = 1.064). It is the highest in perovskites except those metastable compounds needed to be synthesized under high temperature and high pressure conditions. The extremely large lattice distortion is maintained by the strong Pb/Bi-O2 covalency which was evidenced by the experimental investigation on the electron-charge density distribution[30]. However, such giant lattice distortion is significantly reduced by the La substitution (see Supplementary Fig. S4). With increasing La content, the c axis is much reduced, while the $a(b)$ axis is slightly increased. Thus, the c/a is significantly reduced. For example, the originally large c/a of 0.5PT-0.5BL$_x$F is much reduced from 1.14 for the x = 0.0 to 1.057 for the $x = 0.2$. Since the coupling of P_S and lattice is aligned along the c-axis direction, the large decrease in the c axis would imply weakened ferroelectric property. It is worth noting that even though the ionic radius of La^{3+} (1.36 Å) is essentially the same to Bi^{3+} (1.34 Å), the unit cell volume (V) apparently contracts by the substitution of La^{3+} (see Supplementary Fig. S4). The volume contraction is as large as 3.1% by the chemical modification from the x = 0.0 to 0.2. Such large volume contraction should dominate the NTE property.

The temperature evolution of unit cell volume for three compositions of 0.5PT-0.5BL$_x$F (x = 0.0, 0.1, and 0.2) is shown in Fig. 1. It is interesting to observe that the NTE is significantly different from one another. Without the substitution of La, the 0.5PT-0.5BL$_x$F with

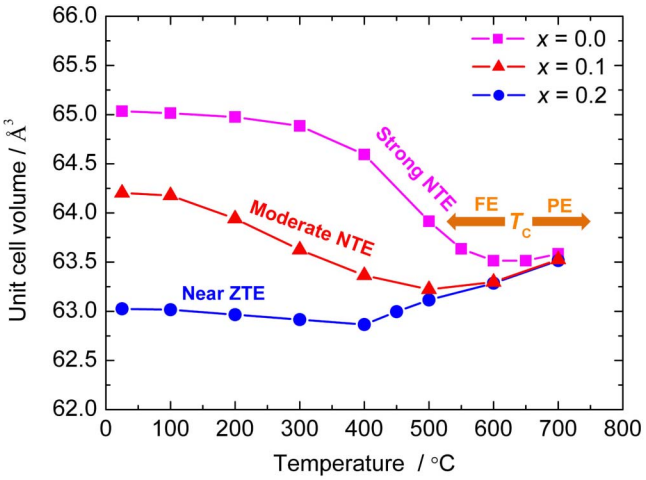

Figure 1 | Negative thermal expansion. Unit cell volume of $0.5PbTiO_3$-$0.5(Bi_{1-x}La_x)FeO_3$ (x = 0.0, 0.1, and 0.2) as function of temperature. FE and PE mean ferroelectric and paraelectric, respectively.

$x = 0.0$ represents a nonlinear and strong NTE in a wide temperature range of RT to 600 °C. It is similar to the composition of 0.4PT-0.6BF near the MPB[23]. In a lower temperature range (RT $\sim$ 300°C), the unit cell volume shows little dependence on temperature with an average bulk CTE of $\alpha_V = -0.83 \times 10^{-5}$°C^{-1}; However, it contracts dramatically at elevated temperatures with $\alpha_V = -7.0 \times 10^{-5}$°C^{-1} (300 $\sim$ 600 °C). The average CTE of the overall temperature range (RT to 600 °C) is $\alpha_V = -4.06 \times 10^{-5}$ °C^{-1}. The contraction of unit cell volume is as giant as -2.3% for the 0.5PT-0.5BL$_x$F ($x = 0.0$). It worth noting that the NTE of 0.5PT-0.5BL$_x$F ($x = 0.0$) is among the giant NTE materials, such as Mn_3AN (-1.3%)[17], $BiNiO_3$ (-2.5 $\sim$ -3.4%)[9], and CuO nanoparticles (-1.1%)[11]. It also needs to note that the present giant NTE in the 0.5PT-0.5BL$_x$F ($x = 0.0$) occurs in a wide temperature range (300 °C) which is broad than other giant NTE materials. For example, $BiNiO_3$ has a colossal NTE over 80 °C[9]; $(Mn_{0.96}Fe_{0.04})_3(Zn_{0.5}Ge_{0.5})N$ shows a giant NTE over 70 °C[17]; and CuO nanoparticles exhibit a giant NTE over 170 °C[11]. It is interesting to observe that the giant NTE of 0.5PT-0.5BL$_x$F can be distinctly weakened by the chemical substitution of La. For the x = 0.1, the NTE becomes linear below T_C with a CTE of $\alpha_V = -3.55 \times 10^{-5}$°C^{-1} (RT $\sim$ 500 °C). With further substitution of La content ($x = 0.2$), the unit cell volume only slightly contracts with increasing temperature. A very low thermal expansion is achieved in a wide temperature range (RT $\sim$ 400 °C). Here, the CTE is $\alpha_V = -0.71 \times 10^{-5}$°C^{-1} for the x = 0.2. We can achieve that the NTE of 0.5PT-0.5BL$_x$F can be tunable over a giant scale of CTE (-7.0 $\sim$ -0.71×10^{-5}°C^{-1}) simply by adjusting La content. It is also important to note that such giant tunable range of CTE contains most known NTE materials[7].

What accounts for such giant-scale control of NTE in the single-phase 0.5PT-0.5BL$_x$F? The NTE of the present 0.5PT-0.5BL$_x$F, which is quantitatively described by the CTE in terms of $\alpha_V = \dfrac{\Delta V}{\Delta T \times V_0}$, is actually dominated by the volume difference, $\Delta V = V_{T_C} - V_{RT}$, where V_{RT} and V_{T_C} are unit cell volumes at RT and T_C, respectively. As shown in Fig. 1, larger absolute value of ΔV means stronger NTE, while smaller one means weakened NTE. It is known that the unit cell volume reaches the minimum value at T_C, due to the fact of NTE in the ferroelectric phase below T_C whereas positive thermal expansion (PTE) in the paraelectric one above T_C. Here, the V_{T_C} is actually dominated by the ionic radius due to the loss of ferroelectricity. Above T_C, the unit cell volume changes linearly, which is originated from lattice thermal vibration. The V_{T_C} of the 0.5PT-0.5BL$_x$F follows to a linear extrapolation of unit cell volume in paraelectric phase.

However, the V_{RT} is strong different from one another. One can see that the strong NTE of the $x = 0.0$ is mainly due to considerably enhanced V_{RT}, while a near ZTE of the $x = 0.2$ is due to significantly reduced V_{RT}. The mechanism of NTE control over such giant scale would be elucidated according to the detailed studies on chemical bonding and hybridization, which will be discussed as follows.

The crystal structure at RT was refined based on Rietveld method by means of neutron powder diffraction. The experimental patterns can be well refined according to tetragonal structure model similar to PT, and atomic positions could be stably calculated. It is known that the equilibrium lattice parameters of ferroelectricity are a balance of short-range repulsion favoring cubic paraelectric phase and long-range Coulomb force favoring ferroelectric one[32]. P_S displacement is a key parameter to represent how ferroelectric property changes in a unit cell. Figure 2 represents the P_S displacements at *A*-site (δz_A) and *B*-site (δz_B) for the 0.5PT-0.5BL$_x$F as function of *x*. They are both reduced at a large content by the substitution of La, indicating a weakened ferroelectric property. For example, the δz_A is reduced from 0.6903 Å of the $x = 0.0$ to 0.4619 Å of the $x = 0.2$ (Supplementary Table S1). The decrease in the P_S displacements should originate from the significantly different ferroelectric activity of Bi and La atoms. It is known that Bi has the strongest ferroelectric activity (0.8 Å), whereas La has a very weak one (0.05 Å)[29]. The La substitution for Bi favors ionic bonding and would weaken the covalent hybridization of cations with oxygens, which can be also reflected from the change in the bond length (see Supplementary Fig. S5). With increasing content of La, chemical bonds of *A*-O2 and *B*-O1 (the shorter one) are elongated, indicating a weakened covalency and hybridization effect. For example, *A*-O2 and *B*-O1 of the $x = 0.0$ are 2.4287 Å and 1.7089 Å, respectively. However, those of the $x = 0.2$ are elongated to 2.5103 Å and 1.8268 Å, respectively. La substitution favors the formation of cubic paraelectric lattice, and weakens the coupling between ferroelectricity and crystal lattice. Actually, there is a strong correlation between the P_S displacement and the *c* axis (see Supplementary Fig. S6). The *c* axis is largely reduced by decreasing P_S displacement. As a result, the V_{RT} of 0.5PT-0.5BL$_x$F is significantly reduced by the La substitution. Thus, the originally giant NTE of 0.5PT-0.5BL$_x$F is strongly weakened by the La substitution.

The effect of La substitution on the covalent hybridization can be further supported by density function theory (DFT) calculation. Two compositions of 0.5PT-0.5BL$_x$F ($x = 0.0$ and 0.25) were calculated in two $2 \times 2 \times 2$ supercells of $(Pb_4Bi_4)(Ti_4Fe_4)O_{24}$ and $(Pb_4Bi_3La_1)(Ti_4Fe_4)O_{24}$, respectively. The degree of hybridization can be quantitatively described by the value of minimum charge density (MED) of specific chemical bonds according to the valence-electron density distribution (Fig. 3). Without La substitution, there is a strong orbital hybridization for the strong NTE composition of 0.5PT-0.5BL$_x$F ($x = 0.0$). The MED value of Bi-O2 bond is as high as 0.45 Å^{-3}. However, the isovalent substitution of La for Bi weakens the hybridization behaviour for all chemical bonds, especially for the chemical bond of Bi-O2. Here, the MED value is reduced to 0.39 Å^{-3} for the composition of $x = 0.25$ which should have a similar low thermal expansion to the $x = 0.2$. The originally strong ferroelectric property cannot well be maintained anymore by the incorporation of weakly ferroelectric active La for strongly ferroelectric active Bi. And thus the P_S displacements are all reduced (Supplementary Table S3). Therefore, due to the fact of much weakened ferroelectricity and a large reduction on the *c* axis, the V_{RT} of the 0.5PT-0.5BL$_x$F significantly shrinks with increasing content of La.

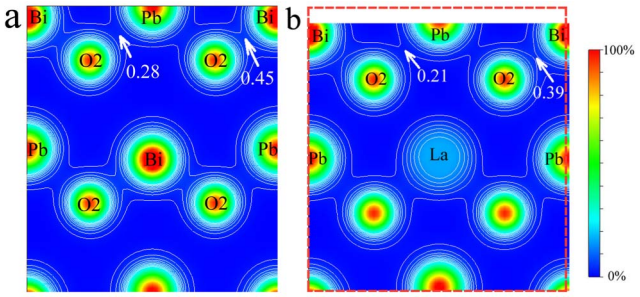

Figure 3 | Valence electron-density distributions on the bc plane at x = 1/2 of supercell. (a) $(Pb_4Bi_4)(Ti_4Fe_4)O_{24}$, and (b) $(Pb_4Bi_3La_1)(Ti_4Fe_4)O_{24}$, which, respectively, corresponds to $x = 0.0$, and $x = 0.25$ of 0.5PbTiO$_3$-0.5(Bi$_{1-x}$La$_x$)FeO$_3$ through first-principle calculations. The dash line frame indicates the original lattice without La substitution. The 0% and 100% in color scale corresponds to 0.2 and 8Å^{-3}, respectively, and contours are from 0.2 to 4 Å^{-3} by step of 0.2 Å^{-3}.

Both detailed studies of crystal structure and first principle calculation have approved that there is a strong correlation between the ferroelectric property and the NTE for the 0.5PT-0.5BL$_x$F. The present results further support the conclusion of the correlation between ferroelectricity and NTE, which was ever revealed by studies of lattice dynamics and temperature dependence of P_S[21,22]. In order for quantitative characterization on the correlation between ferroelectricity and NTE, we introduce a new physical concept of spontaneous volume ferroelectrostriction to represent the contribution from ferroelectric property to NTE. Spontaneous volume ferroelectrostriction is defined as $\omega_s = \frac{V_{exp} - V_{nm}}{V_{nm}} \times 100\%$, where V_{exp} and V_{nm} are, respectively, unit cell volumes of experimental and nominal one. The

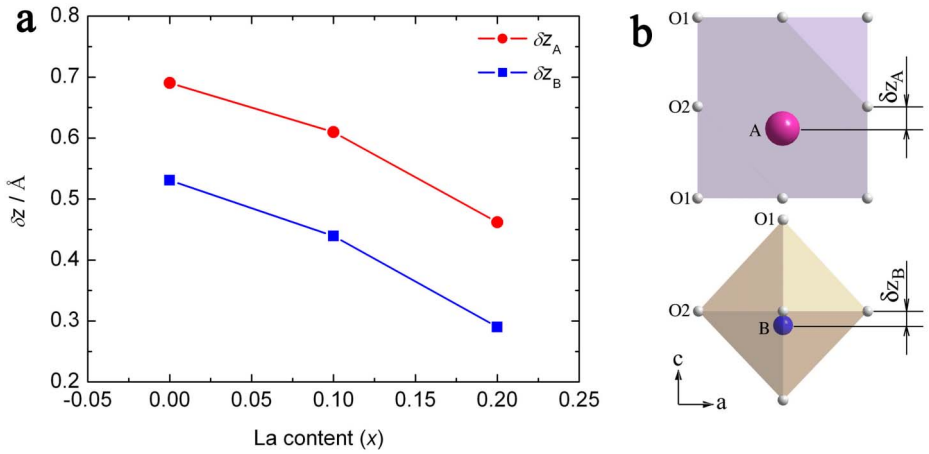

Figure 2 | Spontaneous polarization property. (a) P_S displacements at *A*-site (δz_A) and *B*-site (δz_B) of 0.5PbTiO$_3$-0.5(Bi$_{1-x}$La$_x$)FeO$_3$ as function of La content (*x*). (b) The sketch of P_S displacements of δz_A and δz_B in *A*-O$_{12}$ and *B*-O$_6$ polyhedra, respectively.

nominal one of V_{nm} is calculated by extrapolation from paraelectric to ferroelectric phase. The V_{nm} can be basically considered as the volume component contributed from lattice thermal vibration. Therefore, the volume difference of $V_{exp} - V_{nm}$ represents the quantitative contribution from ferroelectricity. Large value of ω_s means strong NTE, while small one means weak NTE. Similar to Landau theory[33], here we plot the relationship of $\omega_s \sim \alpha\delta z_A^2$ at RT for all investigated compositions of 0.5PT-0.5BL$_x$F, where α is the coupling coefficient between ω_s and P_S (Fig. 4). It is clearly to see that the ω_s shows a good correlation with the square of P_S displacement (δz_A^2). On the one hand, strong ferroelectric property induces a large value of ω_s and thus produces a strong NTE such as for the $x = 0.0$ without La substitution. On the other hand, weakened ferroelectric property induces a small value of ω_s and produces a low thermal expansion such as for the composition of $x = 0.2$.

Discussion

The present study gives a distinct guide to control thermal expansion of ferroelectrics. An effective way to control the NTE would benefit the CTE matching for different components of devices and composites. We can modulate the ferroelectric activity of cations to adjust the value of ω_s and thus control the thermal expansion of ferroelectrics. Strong NTE can be achieved by the substitutions of those cations with strong ferroelectric activity, such as Bi, Ti, Fe, Zn, and Cd, while low thermal expansion by the substitution of cations with weak ferroelectric activity, such as La, Mg, Ni, and Zr[28]. The present study also offers a useful way to achieve ZTE in the family of ferroelectrics. Actually, some of them have been previously experimentally observed to show such ZTE property, such as (Pb,La)TiO_3[34], and well-known ferroelectric relaxor of $Pb(Mg_{1/3}Nb_{2/3})O_3$[15]. It has been known for a long time that perovskite-type Pb-based relaxors exhibit near ZTE below the so-called Burns temperature (T_B)[15,35]. Such near ZTE property could be understood according to the present concept of spontaneous volume ferroelectrostriction. As temperature cooling down from T_B, the effect of spontaneous volume ferroelectrostriction is produced due to the frozen polar nanoregions (PNRs). Therefore, the normal thermal expansion is counteracted and thus near ZTE appears. Future studies could be focused on the precise control and fabrication of ZTE ferroelectric materials for technical application. The NTE control could be also extended to other important functional materials such as multiferroics, since NTE have both strong coupling with not only ferroelectric but also magnetic properties.

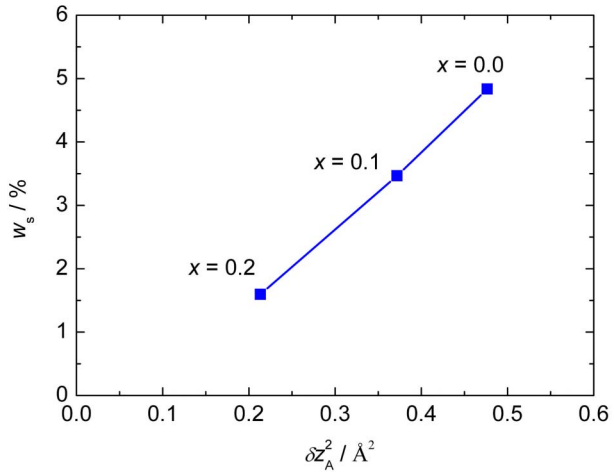

Figure 4 | The correlation between the spontaneous volume ferroelectrostriction (ω_s) and spontaneous polarization. There is a strong correlation of $\omega_s \sim \alpha\delta z_A^2$ for the 0.5PbTiO$_3$-0.5(Bi$_{1-x}$La$_x$)FeO$_3$ ferroelectrics.

In summary, NTE of 0.5PT-0.5BLxF single-phase ferroelectrics is effectively controlled over a giant range from a strong NTE to a near ZTE by the chemical modification. The controllable NTE contains most NTE materials. The details of chemical bonds have been studied by neutron powder diffraction and DFT calculations. The facile control of NTE is strongly correlated to the tunable spontaneous volume ferroelectrostriction by modulating the ferroelectric activity of cations. Present study establishes an effective way to control thermal expansion of functional materials of ferroelectrics.

Methods

Sample preparation. Single-phase materials of 0.5PbTiO$_3$-0.5(Bi$_{1-x}$La$_x$)FeO$_3$ (x = 0.0, 0.1, and 0.2) were prepared by the conventional solid-state reaction method. The following raw materials were used: PbO, Bi_2O_3, TiO_2, La_2O_3, and Fe_2O_3. The well-mixed raw materials were calcined at 750°C for 10 h. Then compacted pellets were sintered at 1100°C for 2 h covered with the powders of the same composition to compensate the loss of PbO and Bi_2O_3 during high temperature sintering process. The surface layers of sintered pellets were removed, and then the sintered pellets were carefully crushed into fine powders.

Structure analysis. Room temperature neutron powder diffraction (NPD) was collected at the NIST Center for Neutron Research on the BT-1 high-resolution neutron powder diffractometer. The wavelength of synchrotron light was 1.5403 Å. The initial structural model of $PbTiO_3$ (space group, *P4mm*) was adopted for the structural refinement performed on software Fullprof. The positions of Pb/Bi/La, Ti/Fe, O1, and O2 are 1*a* site at origin (0,0,0), 1*b* site at (1/2, 1/2, Z_B), 1*b* site at (1/2, 1/2, Z_{O1}), and 2*c* sites at (1/2, 0, Z_{O2})[36], respectively. The high temperature X-ray diffraction (XRD) data were collected on an X-ray powder diffractometer (TTRIII, Rigaku, Japan) using Cu $K\alpha$ radiation. The sample was maintained at a specified temperature for 10 min in order to reach thermal equilibrium. The scanning rate of angle 2θ was 4° min^{-1} and the heating rate was 10°C min^{-1}. The lattice parameters were calculated using the software PowderX and TREOR.

DFT calculation. The electronic structure was calculated based on density functional theory (DFT) with generalized approximations (GGAs) performed with Vienna *ab initio* simulation package (VASP), in order to obtain the valence electron-density distribution of approximated 2 × 2 × 2 supercell of $(Pb_4Bi_4)(Ti_4Fe_4)O_{24}$ and $(Pb_4Bi_3La_1)(Ti_4Fe_4)O_{24}$, corresponding to tetragonal compositions of 0.5PT-0.5BL$_x$F (x = 0.0 and 0.25), respectively.

1. Atkinson, A. *et al.* Advanced anodes for high-temperature fuel cells. *Nat. Mater.* **3**, 17–27 (2004).
2. Tawfick, S. *et al.* Engineering of micro- and nanostructured surfaces with anisotropic geometries and properties. *Adv. Mater.* **24**, 1628–1674 (2012).
3. Haertling, G. H. Ferroelectric ceramics: History and technology. *J. Am. Ceram. Soc.* **82**, 797–818 (1999).
4. Ravi, V. *et al.* Thermal expansion studies of selected high-temperature thermoelectric materials. *J. Electron. Mater.* **38**, 1433–1442 (2009).
5. Mary, T. A., Evans, J. S. O., Vogt, T. & Sleight, A. W. Negative thermal-expansion from 0.3 to 1050 Kelvin in ZrW_2O_8. *Science* **272**, 90–92 (1996).
6. Grigoriadis, C., Haase, N., Butt, H.-J., Müllen, K. & Floudas, G. Negative thermal expansion in discotic liquid crystals of nanographenes. *Adv. Mater.* **22**, 1403–1406 (2010).
7. Evans, J. S. O. Negative thermal expansion materials. *J. Chem. Soc., Dalton Trans.* 3317–3326 (1999).
8. Suzuki, T. & Omote A. Zero thermal expansion in $(Al_{2x}(HfMg)_{1-x})(WO_4)_3$. *J. Am. Ceram. Soc.* **89**, 691–693 (2006).
9. Azuma, M. *et al.* Colossal negative thermal expansion in $BiNiO_3$ induced by intermetallic charge transfer. *Nat. Commun.* **2**, 347 (2011).
10. Mohn, P. A century of zero expansion. *Nature* **400**, 18–19 (1999).
11. Zheng, X. G. *et al.* Giant negative thermal expansion in magnetic nanocrystals. *Nat. Nanotech.* **3**, 724–726 (2008).
12. Holzer, H. & Dunand, D. C. Phase transformation and thermal expansion of Cu/ZrW_2O_8 metal matrix composites. *J. Mater. Res.* **14**, 780–789 (1999).
13. Lommens, P. *et al.* Synthesis and thermal expansion of ZrO_2/ZrW_2O_8 composites. *J. Eur. Ceramic Soc.* **25**, 3605–3610 (2005).
14. Nakajima, N., Yamamura, Y. &Tsujia, T. Synthesis and physical properties of negative thermal expansion materials $Zr_{1-x}M_xW_2O_{8-y}$ (M = Sc, In, Y) substituted for Zr(IV) sites by M(III) ions. *Solid State Commun.* **128**, 193–196 (2003).
15. Roy, R., Agrawal, D. K. & McKinstry, H. A. Very low thermal expansion coefficient materials. *Annu. Rev. Mater. Sci.* **19**, 59–81 (1989).
16. Huang, C. Y., Agrawal, D. K. & McKinstry, H. A. Thermal expansion behaviour of $M'Ti_2P_3O_{12}$ (M′ = Li, Na, K, Cs) and $M''Ti_4P_6O_{24}$ (M″ = Mg, Ca, Sr, Ba) compounds. *J. Mater. Sci.* **30**, 3509–3514 (1995).
17. Takenaka, K. & Takagi, H. Giant negative thermal expansion in Ge-doped anti-perovskite manganese nitrides. *Appl. Phys. Lett.* **87**, 261902 (2005).

18. Iikubo, S., Kodama, K., Takenaka, K., Takagi, H. & Shamoto, S. Magnetovolume effect in $Mn_3Cu_{1-x}Ge_xN$ related to the magnetic structure: Neutron powder diffraction measurements. *Phys. Rev. B* **77**, 020409 (2008).
19. Song, X. Y. *et al.* Adjustable zero thermal expansion in antiperovskite manganese nitride. *Adv. Mater.* **23**, 4690–4694 (2011).
20. Takenaka, K. & Takagi, H. Zero thermal expansion in a pure-form antiperovskite manganese nitride. *Appl. Phys. Lett.* **94**, 131904 (2009).
21. Chen, J. *et al.* Zero thermal expansion in PbTiO3-based perovskites. *J. Am. Chem. Soc.* **130**, 1144–1145 (2008).
22. Chen, J. *et al*. The role of spontaneous polarization in the negative thermal expansion of tetragonal $PbTiO_3$-based compounds. *J. Am. Chem. Soc.* **133**, 11114–11117 (2011).
23. Chen, J., Xing, X. R., Liu, G. R., Li, J. H. & Liu, Y. T. Structure and negative thermal expansion in the $PbTiO_3$-$BiFeO_3$ system. *Appl. Phys. Lett.* **89**, 101914 (2006).
24. Shirane, G. & Takeda, A. Transition energy and volume change at three transitions in barium titanate. *J. Phys. Soc. Jpn.* **7**, 1–4 (1952).
25. Selbach, S. M., Tybell, T., Einarsrud, M.-A. & Grande, T. The ferroic phase transitions of $BiFeO_3$. *Adv. Mater.* **20**, 3692–3696 (2008).
26. Subbarao, E. C. X-ray study of phase $PbNb_2O_6$ and transitions in ferroelectric related materials. *J. Am. Ceram. Soc.* **43**, 439–442 (1960).
27. Chattopadhyayt, T., Boucherlet, J. X. & Schneringt, H. G. von. Neutron diffraction study on the structural phase transition in GeTe. *J. Phys. C: Solid State Phys.* **20**, 1431–1440 (1987).
28. Grinberg, I., Suchomel, M. R., Davies, P. K. & Rappe, A. M. Predicting morphotropic phase boundary locations and transition temperatures in Pb- and Bi-based perovskite solid solutions from crystal chemical data and first-principles calculations. *J. Appl. Phys.* **98**, 094111 (2005).
29. Grinberg, I. & Rappe, A. M. First principles calculations, crystal chemistry and properties of ferroelectric perovskites. *Phase Transit.* **80**, 351–368 (2007).
30. Yashima, M., Omoto, K., Chen, J., Kato, H. & Xing, X. R. Evidence for (Bi,Pb)-O covalency in the high TC ferroelectric $PbTiO_3$-$BiFeO_3$ with large tetragonality. *Chem. Mater.* **23**, 3135–3138 (2011).
31. Sai Sunder, V. V. S. S., Halliyal, A. & Umarji, A. M. Investigation of tetragonal distortion in the $PbTiO_3$-$BiFeO_3$ system by high-temperature X-ray diffraction. *J. Mater. Res.* **10**, 1301–1306 (1995).
32. Cohen, R. E. Origin of ferroelectricity in perovskite oxides. *Nature* **358**, 136–138 (1992).
33. Abrahams, S. C., Kurtz, S. K. & Jamieson, P. B. Atomic displacement relationship to curie temperature and spontaneous polarization in displacive ferroelectrics. *Phys. Rev.* **172**, 551–553 (1968).
34. Chen, J., Xing, X. R., Yu, R. B. & Liu, G. R. Thermal expansion properties of lanthanum-substituted lead titanate ceramics. *J. Am. Ceram. Soc.* **88**, 1356–1358 (2005).
35. Bokov, A. A. & Ye, Z.-G. Recent progress in relaxor ferroelectrics with perovskite structure. *J. Mater. Sci.* **41**, 31–52 (2006).
36. Shirane, G., Pepinsky, R. & Frazer, B. C. X-ray and neutron diffraction study of ferroelectric $PbTiO_3$. *Acta Cryst.* **9**, 131–140 (1956).

Acknowledgements

This work was supported by National Natural Science Foundation of China (Grant Nos. 91022016, 21031005, 21231001), Program for Changjiang Scholars and Innovative Research Team in University (IRT1207), the Foundation for the Author of National Excellent Doctoral Dissertation of PR China (201039), Fok Ying Tung Education Foundation (131047), and Program for New Century Excellent Talents in University (NCET-11-0573). Thanks Prof. Wentong Geng for the supporting on the first-principle calculations.

Author contributions

J.C. and X.R.X. proposed this research and wrote the paper with contributions from all authors. J.C. fabricated the samples and performed the structure refinement analysis. F.F.W. carried out first principle calculations. Q.Z.H. carried out the experiments of neutron powder diffraction and data analysis. X.P.S. and L.H. carried out the experiments of high-temperature XRD and data analysis. J.X.D. and R.B.Y. helped the data analysis and discussion. J.C. and X.R.X. supervised the projects.

Additional information

Supplementary information accompanies this paper at http://www.nature.com/scientificreports

Competing financial interests: The authors declare no competing financial interests.

How to cite this article: Chen, J. *et al.* Effectively control negative thermal expansion of single-phase ferroelecrics of $PbTiO_3$-(Bi,La)FeO_3 over a giant range. *Sci. Rep.* **3**, 2458; DOI:10.1038/srep02458 (2013).

This work is licensed under a Creative Commons Attribution-NonCommercial-NoDerivs 3.0 Unported license. To view a copy of this license, visit http://creativecommons.org/licenses/by-nc-nd/3.0